Lappeenranta University of Technology

School of Engineering Science

Information Technology Program

Bachelor's thesis

**Markus Vartiainen**

# ESTIMATION OF IMAGE LOCAL MEAN NEAR SATURATION

Examiner: Assistant Professor Antti Knutas

Supervisor: Assistant Professor Antti Knutas

# TIIVISTELMÄ

Lappeenrannan teknillinen yliopisto
School of Engineering Science
Tietotekniikan koulutusohjelma

Markus Vartiainen

**Kuvan paikallisen keskiarvon estimointi lähellä saturaatiota**

Kandidaatintyö

2019

33 sivua, 5 kuvaa.

Työn tarkastaja: Apulaisprofessori Antti Knutas

Hakusanat: kuvanprosessointi, kamera, estimointi, kohina, keskiarvo, saturaatio, ylivalotus
Keywords: image processing, camera, estimation, noise, average, mean, saturation, overexposure

Tässä työssä esitetään uusi menetelmä epälineaarisen fotonivasteen korjaamiseksi osittain saturoituneille tasaisille naapurustoille kohinaisissa digitaalikameran kuvissa. Menetelmä perustuu todellisen paikallisen keskiarvon estimointiin liittämällä saturoituneiden pikselien suhteellinen osuus normaalijakautuneeseen kohinaan, korjaten jakauman vinouman, joka aiheutuu joidenkin pikselien saturoitumisesta. Kohina oletetaan normaalijakautuneeksi keskeisen raja-arvolauseen perusteella.

Menetelmällä on potentiaalia lineaarisen suodatuksen, kohinan vähennyksen, värinprosessoinnin ja hahmontunnistuksen parantamiseksi lähellä kuvasignaalin saturoitumisrajaa. Menetelmä on testattu simuloidulla datalla. Päätellään, että työssä esitetty menetelmä toimii hyvin paikallisesti tasaisilla kohteilla, mutta se edellyttää vakiokuvioisen kohinan korjaamista sekä apumenetelmän paikallisen tasaisuuden estimoimiseksi paikallisen keskiarvon aliarvioimisen välttämiseksi. Ehdotuksia menetelmän parantamiseksi käydään läpi.

# ABSTRACT

Lappeenranta University of Technology
School of Engineering Science
Information Technology Program

Markus Vartiainen

**Estimation of image local mean near saturation**

Bachelor's thesis

2019

33 pages, 5 figures.

Examiner: Assistant Professor Antti Knutas

Keywords: image processing, camera, estimation, noise, average, mean, saturation, overexposure

In this thesis a novel method for correcting nonlinear average photon response for partially saturated uniform neighborhoods in noisy digital camera images is presented. The method is based on estimating the true local mean by connecting the ratio of saturated pixels to normally distributed noise, correcting for distribution skewness caused by saturation of some pixels. Normal distributed noise is assumed per central limit theorem.

The method has potential for improving linear filtering, noise reduction, color processing and feature recognition near image signal saturation limit. The method is tested with simulated data. It is concluded that the method presented in the thesis works with locally uniform objects, but it requires correction of fixed-pattern noise and an accompanying method for estimating the degree of local uniformity to prevent undershoot. Suggestions for improving the method are discussed.

## ACKNOWLEDGEMENTS

The work has been done in Tampere for Lappeenranta University of Technology. I want to thank my beloved wife for her understanding and support, my past and present colleagues for sharing their knowledge on this field, my grown-up sons for fruitful discussions on mathematics, and my mother for still providing me a foothold back in Lappeenranta.

Namely, I wish to thank my supervisor, Assistant Professor Antti Knutas for his guidance; my colleague D.Sc. Matti Pellikka for his mentoring and inspiration on mathematics; my colleague M.Sc. Ansse Saarimäki for being my de facto academic opponent for this thesis; and my bosses Janne Haavisto (CTO) and Mika Kuisma (CEO) at Grundium for providing me with the leeway to finish my thesis on time.

My sincerest gratitude goes towards all the helpful people of Lappeenranta University of Technology who made it possible to for me to continue with my postponed academic pursuit.

# TABLE OF CONTENTS

## SYMBOLS AND ACRONYMS

| | |
|---|---|
| $\sim$ | Conforms to (a distribution) |
| $\sim_a$ | Conforms asymptotically to (a distribution) |
| erf | Error function |
| erfc | Complementary error function |
| $\phi$ | PDF of standard normal distribution |
| $\Phi$ | CDF of standard normal distribution |
| $\Phi^{-1}$ | Inverse CDF of standard normal distribution |
| $\mu$ | Expected value |
| $n$ | Total number of pixels |
| $n_{non}$ | Number of non-saturated pixels |
| $n_{sat}$ | Number of saturated pixels |
| $\hat{p}$ | Point estimate for relative number of occurrences |
| $\sigma$ | Standard deviation |
| $\sigma^2$ | Variance |
| $\overline{x}$ | Arithmetic mean of a set of local pixels |
| $\hat{\overline{x}}$ | Estimated local mean of pixels |
| $X$ | Random variable for pixel values |
| $x_{slim}$ | Saturation limit value |
| $z$ | Normalized value |
| $\hat{\overline{z}}$ | Normalized estimated local mean of pixels |
| $Z$ | Normalized random variable for pixel values |
| $z_{slim}$ | Normalized saturation limit value |

| | |
|---|---|
| BLC | Black level correction |
| CC | Color correction |
| CCD | Charge-coupled device |
| CDF | Cumulative distribution function |
| CDS | Correlated double sampling |
| CE | Contrast enhancement |
| CFAI | Color filter array interpolation |
| CNR | Color noise reduction |

| | |
|---|---|
| DPC | Defective pixel correction |
| CMOS | Complementary metal-oxide semiconductor |
| DCSN | Dark current shot noise |
| DN | Digital number |
| DSNU | Dark signal nonuniformity |
| EC | Exposure correction |
| FPN | Fixed pattern noise |
| GE | Gamma encoding |
| PDF | Probability density function |
| PRNU | Photon response nonuniformity |
| PSN | Photon shot noise |
| RNR | Raw noise reduction |
| SC | Shading correction |
| TN | Temporal noise |
| WB | White balance |

# 1 INTRODUCTION

Overexposure is a well-known phenomenon with digital cameras. It happens when an image, or part of it, gets more light than individual pixels can measure. Local overexposure typically happens with high-contrast scenes, e.g. with presence of a light source or an object under bright illumination, such as a cloud on a sunny day. Each pixel can count only certain number of incident photons before it gets saturated, and beyond that point there is no telling how many photons actually arrived [1; 2; 3; 4; 5; 6]. Even when a pixel is not saturated, it is impossible to tell exactly what would have been the real expected number of incident photons from the object for that particular pixel because of noise. A major component of image noise comes from the light itself as photon shot noise (PSN). Emittance of photons is a Poisson process, which means that the number of emitted photons over a time unit is a random variable with Poisson distribution. [1; 2; 4; 5].

Near saturation, noise causes some pixels to randomly saturate and some to not saturate despite their real expected values. At the saturation limit, on average half of the pixels will randomly saturate, while the other half stays at random values below saturation limit. This causes the noise distribution to skew towards lower values, resulting in an undershoot of the local mean. Formation and appearance of a noisy digital camera image with PSN at saturation limit is illustrated in Figure 1.1. Batches of randomly darkened pixels are clearly separated from a saturated white background, giving an overall greyish appearance to the image that would otherwise be perfectly white.

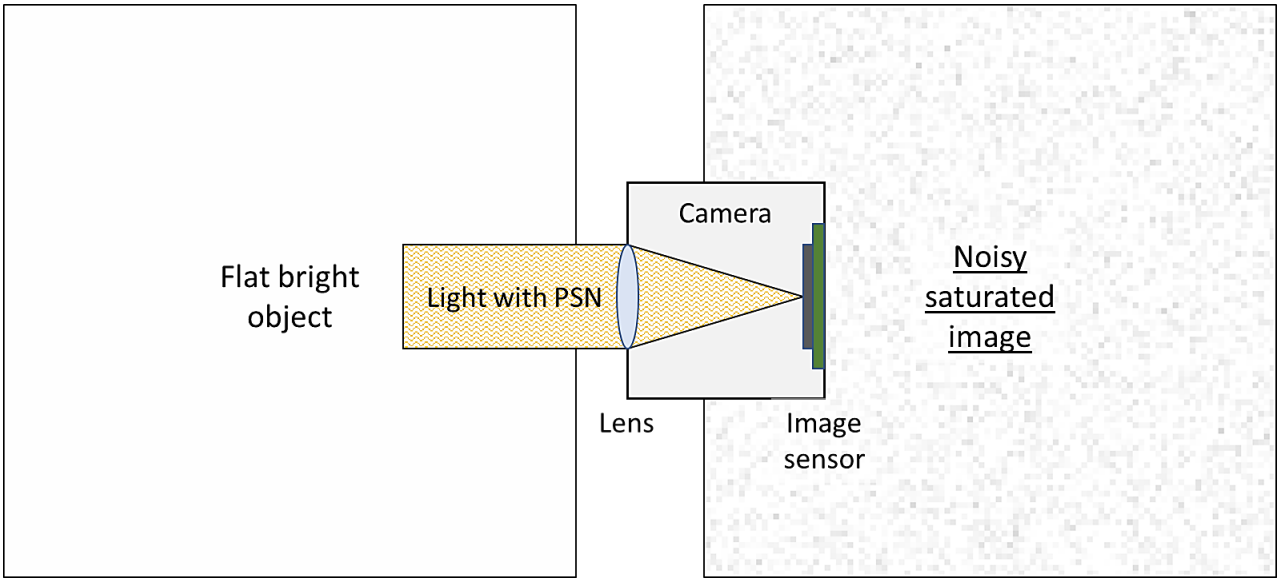


**Figure 1.1: Appearance of a flat object at saturation limit in a noisy digital camera image.**

Within a neighborhood where the expected intensity of light is uniform, the expected intensity can be estimated as the arithmetic mean of intensities of neighboring pixels [7]. This as such is a good estimate for a sufficiently large neighborhood, as far as there are no saturated pixels within that neighborhood. Without saturated pixels, the signal average follows incoming intensity in linear fashion. However, near saturation limit, the increase of recorded signal turns nonlinear due to some of the noisy pixel values being saturated and clipped. Only somewhat far beyond the saturation limit the where increase stops entirely and stays flat [1; 2; 4; 5].

Noise-originating signal nonlinearity is illustrated in Figure 1.2, where signal mean and variance are calculated from a series of simulated noisy flat images of increasing intensity. For simplicity, the number of simulated photons is chosen to be the same as the resulting digital number, and the noise is Poisson-distributed. The saturation limit is chosen to be at signal level 511. When approaching the saturation limit, the increase of actual average signal starts to slow down, reaching the saturation value only after passing significantly beyond the theoretical saturation intensity. Similarly, after a steady increase, noise variance starts falling near saturation as more and more pixels get saturated and lose their randomness, eventually reaching zero when the signal is so oversaturated that there is no practical chance for a pixel to have a low enough value to not get saturated.

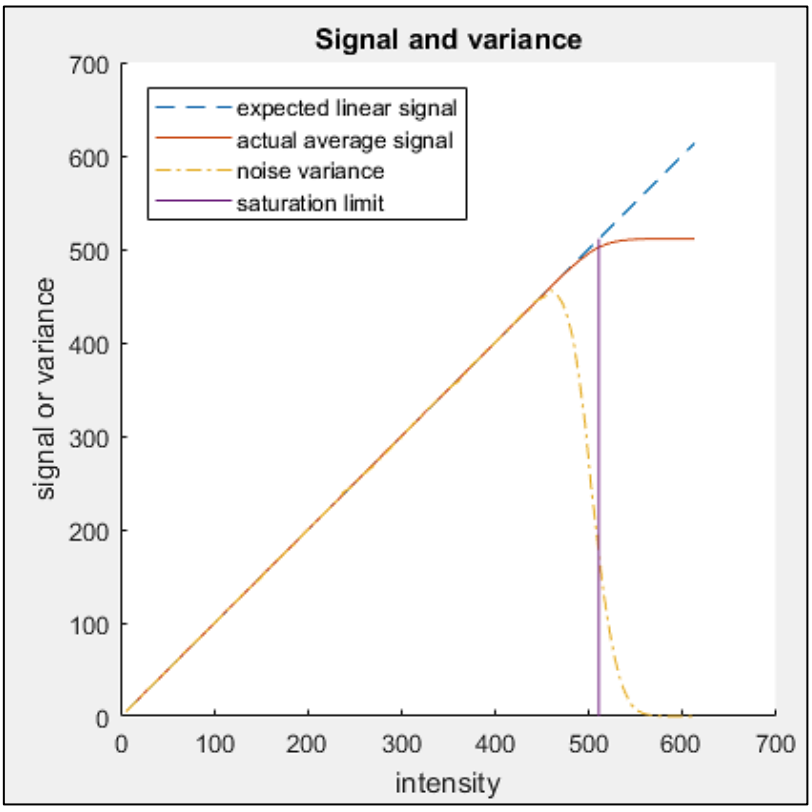


**Figure 1.2: Signal and its noise variance as function of incoming intensity.**

## 1.1 Purpose

This thesis presents a method for estimating the local mean when some pixels within a uniform neighborhood are saturated. It is possible to estimate the local mean even beyond saturation limit as far as not all pixels are saturated.

The method presented in this thesis can be used to improve image processing methods that rely on a good estimate of local mean, e.g.

- linear spatial filtering
- noise reduction
- feature recognition, and
- color processing,

when the local neighborhood is partially saturated and represents a uniform object.

A linear spatial filter smoothens an image by replacing image points with their local mean [8]. It can be used e.g. for simple noise reduction and imitation of the Bokeh effect (optical background blur) [9]. Local average intensity can be used for adjusting noise filter strength [10]. In feature recognition, local variance can be used to estimate presence of details [8], and calculation of mean is a necessary for calculation of variance [7]. Color processing can be improved through improved linearization of the image signal near saturated objects [3; 11].

The phenomenon examined in this thesis occurs in all digital image sensors. It is especially relevant for mobile cameras, where dynamic range is limited by small pixel size [1].

Production of digital image sensors today is massive. The two leading types of digital image sensors are complementary metal-oxide semiconductor (CMOS) and charge-coupled device (CCD) image sensors. The number of CMOS image sensors alone shipped in 2019 is predicted to be 6.1 billion ($6.1 \times 10^9$) [12]. The number of smartphones (each typically employing at least two small CMOS image sensors) sold in 2018 was about 1.6 billion [13]. The number of interchangeable lens cameras (which usually employ a large image sensor) shipped has been declining and in 2018 has been merely about 11 million ($11 \times 10^6$) and the number of built-in cameras about 8.6 million ($8.6 \times 10^6$) units [14], so while about half of the CMOS image sensors go to smartphones, the other half is employed in other imaging applications e.g. in the industrial, security and automotive sectors.

## 1.2 Targets and limitations

The target of this thesis is to establish a method for estimating the local average signal from partially saturated single-channel image data, based on understanding of image noise as found in literature.

Analysis is limited to the nonlinearity caused by noise behavior near saturation limit within a single dominant color channel. Other causes of nonlinearity are ignored. Color imaging is not considered. Concrete implementation of the method is limited to simulation. A simplified noise model, resting on the central limit theorem, will be used in order to separate the core phenomenon from the intricacies of real noise in digital cameras.

## 1.3 Research method

The research method for this thesis is simulation. An understanding of behavior of image noise and related mathematical statistics will be based on a literature. Simulated image data will be generated per this understanding, and the developed method will be tested on the simulated data.

## 1.4 Structure of the work

Chapter *Introduction* lays the purpose of the work and sets the targets and limitations. Research method and structure of the work are discussed.

Chapter *Background* sets a context for the research question. Basis for the model is established.

Chapter *Method* contains the major contribution of the work, presenting a method for estimation of image local mean under partial saturation.

Chapter *Results* shows how the method is used for estimating image local mean per the model with simulated data.

Chapter *Discussion* evaluates the meaning of the results and considers options for further steps.

Chapter *Conclusions* summarizes the work.

# 2 BACKGROUND

In this chapter, an understanding of digital camera systems and sources of image noise is established. Digital camera systems, sources of image noise, and characterization of digital cameras are studied.

## 2.1 Digital camera systems

[1] provides an overview of digital camera systems. Here, a summary of that, combined to author's own experience on the field, is provided.

A digital camera system typically consists of:

- lens system
- (focusing mechanism)
- (adjustable iris)
- (shutter)
- (infrared filter)
- image sensor, consisting of
    - photosites
    - analog circuitry
    - analog-to-digital converter
    - digital circuitry
- digital image signal processor
- system controller
- data interfaces
- (image encoder)
- (video encoder)
- (display)

Building a camera starts with a dark chamber, which limits incoming light so that it only gets in through well-defined opening and provides housing for the other parts of the camera: the lens system, through which the light travels and which creates an image of the object at the back of the camera; the focusing mechanism, which moves the lens further from or closer to the image sensor to focus the camera system to an object at certain distance; an adjustable iris which ultimately decides how much

light is allowed into the lens; a shutter which is opened to expose the image sensor for capturing light, and the image sensor.

A modern lens system consists of several lens elements, together forming a compound lens. The capability of a single lens to form a good image is limited, and lenses are added to balance optical aberrations so that a high-quality image is formed throughout the field. Often the lens system is referred to as just “lens” when the details of implementation are not considered relevant.

The image sensor consists of light-sensitive photosites, analog circuitry for preprocessing and collecting signal from the photosites, an analog-to-digital converter and digital circuitry to interface with rest of the digital electronics.

A digital image signal processor, although strictly speaking not mandatory, is an essential part in creating a proper image from the raw image data, which as such is by no means unusable, but does not adhere to even modest expectations of a proper image. To create such a proper image, the following steps are taken by the image signal processor:

- defective pixel correction (DPC)
- raw noise reduction (RNR)
- black level correction (BLC)
- shading correction (SC)
- color filter array interpolation (CFAI)
- white balancing (WB)
- exposure correction (EC)
- color conversion (CC)
- color noise reduction (CNR)
- contrast enhancement (CE)
- gamma encoding (GE)

All cameras have defective pixels, and their signal have to be replaced with e.g. values interpolated from their neighborhood.

Some noise reduction is usually done to the raw image before further processing, because at this point the noise is intact and most faithfully reflects its behavioral model.

Shading comes in many forms and may be caused e.g. by extreme field angles in the image side or details of the image sensor electronics such as placement of heat-generating circuitry.

Color filter array interpolation (CFAI) is done for color sensors, which have a color filter mosaic on top of the photosites to create a subsampled version of the image on different colors; typically red, green and blue. The result of CFAI is a full resolution image on all color channels.

White balancing adjusts the color components with relation to each other so that white looks white and grey looks grey in the result. This is because the color filters in the camera don't correspond to the spectral sensitivity of the human eye very accurately, and the human vision also adapts to color of the illumination to some extent.

Exposure correction means digital gain, which is used to boost the brightness of an image with low exposure. Low exposure might be caused by low illumination, when reasonable exposure time has reached its maximum (which could happen to avoid excessive motion blur).

Colors must be converted from the color space of the camera to a standard color space which is designed for display to humans. This is because of the color filters in the camera don't correspond to the spectral distribution of the human eye.

Color noise reduction can be made once the raw color mosaic image has been converted to multi-channel color image. Color noise looks odd and disturbing to human eye, but then again human vision sticks more to details than colors. Thus, it makes sense to reduce the amount of color noise without touching detail, using color space which allows for separation of the two, such as the CIELAB color space [15].

Contrast enhancement is done depending on application. Usually high-contrast images please the eye of the consumer, but an industrial application may not do any contrast enhancement by default since it does not increase the amount of information in the image.

Gamma encoding is made last to conform to the modern display standards and to provide more granularity to dark levels, for which the human vision has better resolution than to the bright levels due to the Weber-Fechner logarithmic law [4].

Of these, color related steps are not done in case of monochromatic imaging, such as some industrial imaging cases.

In some cameras, focus is fixed so they don't include focusing mechanism. Small digital cameras, such as mobile cameras, typically don't have adjustable iris or mechanical shutter; a fixed iris and an electronic shutter are used instead. Infrared filter is needed for general purpose cameras, which may receive plenty of human-invisible infrared radiation which would end up as unexpected color intensity. Image and video encoders are not a mandatory part of a digital camera system, but usually there is a reason to have them. Finally, the camera system itself might not have a display, but eventually the images will be shown on some display somewhere.

## 2.2 Sources of image noise

[1] provides an overview of image noise sources. Here, a summary is presented.

Noise in image sensors can be divided to two categories per their behavior:

- fixed pattern noise (FPN), and
- temporal noise (TN).

FPN does not vary over time, and it always affects the image the same way. Some FPN is spatially random (such as weak pixels and leakers), while some is spatially correlated (such as column or row FPN). FPN may have electronic or optical origin.

TN varies randomly over time, and each pixel can be considered to vary independently from each other. When a snapshot is taken, the temporal noise is "frozen" into random spatial noise, but this spatial noise in subsequent frames has no correlation to each other.

FPN and TN can both be divided to two categories per their occurrence:

- dark noise (occurring in darkness)
- light noise (occurring under illumination)

Dark FPN is dark signal nonuniformity (DSNU) and light FPN is photon response nonuniformity (PRNU).

Dark TN is dark current shot noise (DCSN), which originates from random events occurring in the image sensor semiconductor. Light TN is photon shot noise (PSN), and it originates from the light source.

Both the random events regarding DCSN and the emittance of photons are Poisson processes, which means that

1) they occur independently on some average but random intervals with exponential distribution, and thus
2) they accumulate over a time unit with some average but random number of occurrences, following Poisson distribution.

DCSN cumulates over time, and is significant with long exposures and low signals. PSN depends on the number of incident photons, and is while in high signals its absolute amount is greater, it's relative amount in comparison to the signal is lower. That is, signal-to-noise ratio (SNR) of high signal with PSN is better than that of a low signal with PSN. Both DCSN and PSN have their greatest impact on the image quality when high gains are used to compensate for low exposure (in e.g. low light situations).

Additionally there are noise sources related to resetting and reading pixel values, caused solely by the electronics.

Image sensors also generate flicker noise or 1/f noise, which causes periodic low-frequency fluctuation in pixel values. It is called 1/f noise, because its amplitude is inversely related to its frequency. It has electronical origin, but its generation mechanism is not well understood. Flicker noise is usually suppressed by using correlated double sampling (CDS). In CDS, the pixel is reset immediately after reading its value, and the value is read again. The output value is the difference between the values before and after readout and reset [1].

## 2.3 Characterization of camera noise

[2] provides a comprehensive treatment for camera characterization. Here, a summary is presented.

Camera characterization can be presented as a family of photon transfer curves (PTC). A PTC manifests the standard deviation of one or more noise contributors as a function of signal. Noise contributors are:

- read noise
- shot noise
- FPN
- combinations of above

A PTC can be expressed in units of electrons ($e^-$) or digital numbers (DN). Measurement is made in units of DN and converted to $e^-$. Measurement is made from a suitable patch in the middle of the image of a flat object. This is done for a series of images which represent increasing signal level. Increasing signal level can be achieved by varying exposure time.

A PTC is divided to four regimes, ordered from low to high signal:

1. read noise regime
2. shot noise regime
3. FPN regime
4. full regime

Read noise regime consists of zero signals, where noise originates solely from signal handling. This includes multiple noise sources related to the electronical implementation of pixels.

Shot noise regime consists of low signals, where noise originating from photons dominates. This is Poisson-distributed noise, and its standard deviation increases as square root of signal (in $e^-$).

FPN regime takes over the shot noise regime as signal increases, because it scales linearly with signal (in $e^-$).

Full regime starts from saturated signal. Near saturation limit, the increase of noise standard deviation starts to slow down due to clipping of noise as the number of randomly saturated (and thus constant) pixels increases. Eventually, the noise standard deviation starts decreasing and approaches zero asymptotically.

Noise characterization is done by following steps:

1. Removal of dark fixed pattern noise. This happens by averaging several dark frames, resulting in a single frame with almost entirely of dark FPN. (The more frames are averaged, the lower is the contribution of dark TN.)
2. Calculation of average signal per signal level. This happens by subtracting the dark average frame from each frame that represent different exposures, and averaging the result into single signal value per exposure.

3. Calculation of total noise per signal level. This happens by calculating variance for each frame (of different exposure time) by taking the square root of the mean of the squares of the differences of each pixel value and frame average. This value contains both TN and FPN.

Additionally, contribution of FPN can be eliminated by taking two identical frames back-to-back for each exposure time, subtracting one from another and calculating squared mean of the average and taking square root to yield standard deviation. This result has to be further divided by $\sqrt{2}$ to adjust for the increase of random noise due to application of two noisy frames instead of just one. This, finally, yields the contribution of the TN only.

# 3 METHOD

In this chapter, a novel method for estimation of local mean under partial saturation is presented.

The model assumes that noise statistical distribution near saturation follows approximately the normal distribution, per central limit theorem. It is also assumed that the object is locally uniform.

Noise sources accumulate creating total noise that consists of FPN and TN. FPN can be compensated by bias removal and pixel gains based on sensor characterization. TN accumulates towards normally distributed distribution per central limit theorem [7]. As PSN follows Poisson distribution and near saturation its expected value is in thousands (in $e^-$) [1], it can be accurately approximated with normal distribution [7].

## 3.1 Estimation of local mean under partial saturation

With no saturated pixels within a neighborhood, the local mean (a sample mean) is

$$\overline{x} = \frac{\sum_{i=1}^{n} x_i}{n}, \qquad n_{sat} = 0 \tag{3.1}$$

where $\overline{x}$ is the local mean, $n$ is the number of pixels within the neighborhood, and $x_i$ are the signal values within the neighborhood [7; 8].

When saturated pixels are present within a neighborhood, the estimated local mean is a sum of the mean of the non-saturated pixels within the neighborhood and the estimated mean of the saturated pixels within the neighborhood, weighted by their corresponding relative numbers:

$$\hat{\overline{x}} = \frac{n_{non}\overline{x}_{non} + n_{sat}\hat{\overline{x}}_{sat}}{n}, \qquad n_{sat} > 0 \tag{3.2}$$

where

- $\hat{\overline{x}}$ is the estimated local mean,
- $\overline{x}_{non}$ is the mean of the non-saturated pixels,
- $\hat{\overline{x}}_{sat}$ is the estimated mean of the saturated pixels,
- $n_{non}$ is the number of non-saturated pixels,
- $n_{sat}$ is the number of saturated pixels, and
- $n$ is the total number of pixels within the neighborhood.

Per equation 3.1, the mean of non-saturated pixels is

$$\overline{x}_{non} = \frac{\sum_{i=1}^{n_{non}} x_i}{n_{non}} \tag{3.3}$$

Substituting this to 3.2, $n_{non}$ can be eliminated:

$$\hat{\overline{x}} = \frac{\sum_{i=1}^{n_{non}} x_i + n_{sat}\hat{\overline{x}}_{sat}}{n} \tag{3.4}$$

The number of non-saturated pixels can be expressed as sum of occurrences:

$$n_{non} = \sum_{i=1}^{n} \begin{cases} 1, & x_i < x_{slim} \\ 0, & \text{otherwise} \end{cases} \tag{3.5}$$

where $x_{slim}$ is the saturation limit value.

The number of saturated pixels is the complement of this:

$$n_{sat} = n - n_{non} \tag{3.6}$$

The mean of the saturated pixels cannot be calculated per se, as that information is lost in saturated signals. However, it can be estimated by assuming that

- the object present in the neighborhood is nearly uniform, and
- the number of saturated pixels follows normal distribution.

Figure 3.1 illustrates the statistical distribution of saturated pixels within a partially saturated neighborhood. Horizontal axis represents pixel values (adjusted for true local mean), vertical axis represents number of pixels, and $x_{sat}$ marks the saturation limit value. The right part under the curve contains the saturated portion of the neighborhood.

The method of estimating local mean under partial saturation is based on this idea.

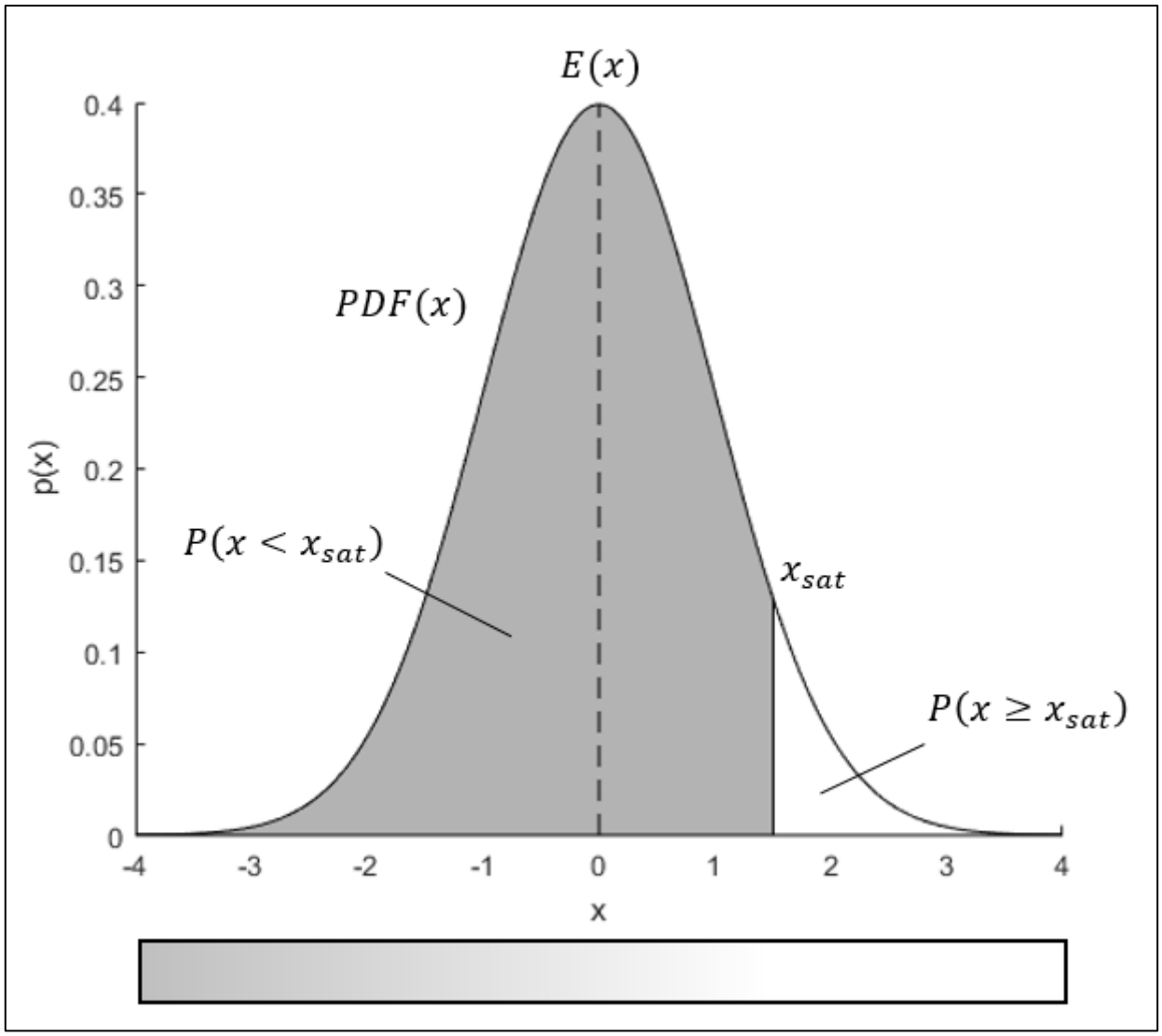


**Figure 3.1: Probability of saturated signal for given expected signal level, saturation level and probability distribution.**

Let the signal values within the neighborhood be represented by a random variable $X$ which follows normal distribution:

$$X \sim N(\mu, \sigma^2) \tag{3.7}$$

where $\mu$ is the expected value of the neighborhood and $\sigma^2$ is the variance of the neighborhood.

A point estimate $\hat{p}$ of the relative number of saturated pixels within the neighborhood is given by

$$\hat{p} = \frac{n_{sat}}{n} \tag{3.8}$$

and it can be said that the probability that a pixel within the neighborhood is saturated, is approximately this point estimate:

$$P(X \geq x_{slim}) \approx \hat{p} \tag{3.9}$$

The normal distribution has a probability density function (PDF)

$$f(x) = \frac{1}{\sigma\sqrt{2\pi}} e^{\frac{-(x-\mu)^2}{2\sigma^2}} \tag{3.10}$$

for $-\infty \leq x \leq \infty$, where $x$ is a random value [16].

For standard normal distribution $\phi(z)$, $\mu = 0$ and $\sigma = 1$, and the PDF simplifies to

$$\phi(z) = \frac{1}{\sqrt{2\pi}} e^{\frac{-z^2}{2}} \tag{3.11}$$

for $-\infty \leq z \leq \infty$, where $z$ is a normalized random value [7].

Random variable $X$ can be normalized so that it follows standard normal distribution by

$$Z = \frac{X - \mu}{\sigma} \tag{3.12}$$

where $Z$ is the normalized random variable [7].

Individual random value $x$ is normalized similarly by

$$z = \frac{x - \mu}{\sigma} \tag{3.13}$$

where $z$ is the normalized random value.

The point estimate for relative number of saturated pixels within the neighborhood is the same for both normalized and real standard distribution. Thus

$$1 - \Phi(z_{slim}) = \hat{p} \tag{3.14}$$

$$\Phi(z_{slim}) = 1 - \hat{p} \tag{3.15}$$

where $z_{slim}$ is the normalized saturation limit value, and $\Phi$ is the standard normal cumulative distribution function (CDF).

Standardized saturation limit value can be solved with an inverse of the standard normal CDF $\Phi^{-1}$:

$$z_{\text{slim}} = \Phi^{-1}(1 - \hat{p}) \tag{3.16}$$

For a locally uniform object, the estimated mean of the saturated signal values is the 1) integral of the normal probability density function 2) for values above the saturation limit, 3) weighted by the corresponding values and 4) normalized by the probability of those values [16]:

$$\hat{\bar{x}}_{sat} = \frac{\int_{x_{slim}}^{\infty} x\, f(x)\, dx}{\int_{x_{slim}}^{\infty} f(x)\, dx} \tag{3.17}$$

Because saturation limit $z_{slim}$ is known, the standard normal distribution function can be used to obtain normalized mean of the saturated signal values:

$$\hat{\bar{z}}_{sat} = \frac{\int_{z_{slim}}^{\infty} z\, \phi(z)\, dz}{\int_{z_{slim}}^{\infty} \phi(z)\, dz} \tag{3.18}$$

Substituting $\phi(z)$ with equation 3.11,

$$\hat{\bar{z}}_{sat} = \frac{\int_{z_{slim}}^{\infty} z \frac{1}{\sqrt{2\pi}} e^{\frac{-z^2}{2}}\, dz}{\int_{z_{slim}}^{\infty} \frac{1}{\sqrt{2\pi}} e^{\frac{-z^2}{2}}\, dz} \tag{3.19}$$

Carrying out the integration,

$$\hat{\bar{z}}_{sat} = \frac{\sqrt{\frac{2}{\pi}} e^{\frac{-z_{slim}{}^2}{2}}}{\text{erfc}\left(\frac{z_{slim}}{\sqrt{2}}\right)} \tag{3.20}$$

where $z_{slim}$ is the normalized saturation limit as given by equation 3.16, and the complementary error function erfc is special function [16]

$$\mathrm{erfc}(x) = 1 - \mathrm{erf}(x) = \frac{2}{\sqrt{\pi}} \int_x^{\infty} e^{-t^2}\, dt \tag{3.21}$$

Because

$$\phi(x) = \frac{1}{\sqrt{2\pi}} e^{\frac{-x^2}{2}} \tag{3.22}$$

the nominator can be expressed as

$$\sqrt{\frac{2}{\pi}} e^{\frac{-z_{slim}{}^2}{2}} = \sqrt{\frac{2}{\pi}} \sqrt{2\pi} \frac{1}{\sqrt{2\pi}} e^{\frac{-z_{slim}{}^2}{2}} = \sqrt{\frac{2}{\pi}} \sqrt{2\pi} \phi(z_{slim}) = 2\phi(z_{slim}) \tag{3.23}$$

which, substituted to equation 3.20, gives

$$\hat{\bar{z}}_{sat} = \frac{2\phi(z_{slim})}{\mathrm{erfc}\left(\frac{z_{slim}}{\sqrt{2}}\right)} \tag{3.24}$$

Per [7], the normalized mean of saturated pixels can be expressed as a function of real mean of saturated pixels:

$$\hat{\bar{z}}_{sat} = \frac{\hat{\bar{x}}_{sat} - \mu}{\sigma_{slim}} \tag{3.25}$$

From this, the real mean of saturated pixels can be solved:

$$\hat{\bar{x}}_{sat} = \sigma_{slim} \hat{\bar{z}}_{sat} + \mu \tag{3.26}$$

By substituting $\hat{\bar{z}}_{sat}$ from equation 3.24, it is obtained that the estimated mean of the saturated pixels is

$$\hat{\bar{x}}_{sat} = \sigma \frac{2\phi(z_{slim})}{\mathrm{erfc}\left(\frac{z_{slim}}{\sqrt{2}}\right)} + \mu. \tag{3.27}$$

Per equation 3.16, $z_{slim}$ is readily known by the point estimate of relative number of saturated pixels.

Substituting this to the formula for estimated local mean (equation 3.2) and replacing the expected value $\mu$ is with the estimated mean itself, the following formula is obtained:

$$\hat{\bar{x}} = \frac{n_{non}\bar{x}_{non} + n_{sat}\left(\sigma \frac{2\phi(z_{slim})}{\operatorname{erfc}\left(\frac{z_{slim}}{\sqrt{2}}\right)} + \hat{\bar{x}}\right)}{n} \tag{3.28}$$

Solve for $\hat{\bar{x}}$. Open parentheses:

$$\hat{\bar{x}} = \frac{n_{non}\bar{x}_{non} + n_{sat}\sigma \frac{2\phi(z_{slim})}{erfc\left(\frac{z_{slim}}{\sqrt{2}}\right)} + n_{sat}\hat{\bar{x}}}{n} \tag{3.29}$$

Move all $\hat{\bar{x}}$ to the left:

$$\hat{\bar{x}} - \frac{n_{sat}}{n}\hat{\bar{x}} = \frac{n_{non}\bar{x}_{non} + n_{sat}\sigma \frac{2\phi(z_{slim})}{\operatorname{erfc}\left(\frac{z_{slim}}{\sqrt{2}}\right)}}{n} \tag{3.30}$$

Take $\hat{\bar{x}}$ out:

$$\hat{\bar{x}}\left(1 - \frac{n_{sat}}{n}\right) = \frac{n_{non}\bar{x}_{non} + n_{sat}\sigma \frac{2\phi(z_{slim})}{\operatorname{erfc}\left(\frac{z_{slim}}{\sqrt{2}}\right)}}{n} \tag{3.31}$$

Divide by the $\hat{\bar{x}}$ multiplier:

$$\hat{\bar{x}} = \frac{n_{non}\bar{x}_{non} + n_{sat}\sigma \frac{2\phi(z_{slim})}{\operatorname{erfc}\left(\frac{z_{slim}}{\sqrt{2}}\right)}}{n\left(1 - \frac{n_{sat}}{n}\right)} \tag{3.32}$$

Open parentheses:

$$\hat{\bar{x}} = \frac{n_{non}\bar{x}_{non} + n_{sat}\sigma \frac{2\phi(z_{slim})}{\operatorname{erfc}\left(\frac{z_{slim}}{\sqrt{2}}\right)}}{n - n_{sat}} \tag{3.33}$$

Substitute $\bar{x}_{non}$ with equation 3.3:

$$\hat{\bar{x}} = \frac{n_{non}\frac{\sum_{i=1}^{n_{non}} x_i}{n_{non}} + n_{sat}\sigma\frac{2\phi(z_{slim})}{\text{erfc}\left(\frac{z_{slim}}{\sqrt{2}}\right)}}{n - n_{sat}} \tag{3.34}$$

Simplify first term, cancelling $n_{non}$:

$$\hat{\bar{x}} = \frac{\sum_{i=1}^{n_{non}} x_i + n_{sat}\sigma\frac{2\phi(z_{slim})}{\text{erfc}\left(\frac{z_{slim}}{\sqrt{2}}\right)}}{n - n_{sat}} \tag{3.35}$$

Substitute $n - n_{sat} = n_{non}$ from equation 3.6:

$$\hat{\bar{x}} = \frac{\sum_{i=1}^{n_{non}} x_i + n_{sat}\sigma\frac{2\phi(z_{slim})}{\text{erfc}\left(\frac{z_{slim}}{\sqrt{2}}\right)}}{n_{non}} \tag{3.36}$$

Distribute divider to terms:

$$\hat{\bar{x}} = \frac{\sum_{i=1}^{n_{non}} x_i}{n_{non}} + \frac{n_{sat}2\sigma\phi(z_{slim})}{n_{non}\text{erfc}\left(\frac{z_{slim}}{\sqrt{2}}\right)} \tag{3.37}$$

Substitute first term with $\bar{x}_{non}$:

$$\hat{\bar{x}} = \bar{x}_{non} + \frac{2n_{sat}\sigma\phi(z_{slim})}{n_{non}\text{erfc}\left(\frac{z_{slim}}{\sqrt{2}}\right)} \tag{3.38}$$

Finally, substitute $\sigma$ with the characterized noise standard deviation at saturation limit, $\sigma_{slim}$ obtained from camera characterization:

$$\hat{\bar{x}} = \bar{x}_{non} + \frac{2n_{sat}\sigma_{slim}\phi(z_{slim})}{n_{non}\text{erfc}\left(\frac{z_{slim}}{\sqrt{2}}\right)} \tag{3.39}$$

where $z_{slim} = \Phi^{-1}(1-\hat{p}) = \Phi^{-1}\left(1 - \frac{n_{sat}}{n}\right)$ per equations 3.16 and 3.8.

For completeness, the estimate when there are no saturated pixels, some saturated pixels, or all saturated pixels is

$$\hat{\bar{x}} = \begin{cases} \bar{x}_{non}, & n_{sat} = 0 \\ \bar{x}_{non} + \dfrac{2n_{sat}\sigma_{slim}\phi(z_{slim})}{n_{non}\mathrm{erfc}\left(\dfrac{z_{slim}}{\sqrt{2}}\right)}, & 0 < n_{sat} < n \\ \infty, & n_{sat} = n \end{cases} \tag{3.40}$$

i.e. the estimate is the mean of non-saturated pixels when there are no saturated pixels present; infinity when all pixels are saturated, and the obtained result for partial saturation.

Equation 3.40 is the final form of the estimate for the local mean of a locally uniform object under partial saturation.

# 4 RESULTS

In Figure 4.1 experimental results with uniform image and simulated Poisson noise are presented for 100×100, 10×10, 5×5 and 3×3 pixel rectangular neighborhoods. Signal is set equal to incoming intensity and is perfectly linear except for noise and saturation. Noise variance is set equal to signal level in DN, (standard deviation being square root of the variance). In each case, the estimated signal level (per equation 3.40) follows the linear intensity, although there is increasing amount of variation as the window size gets smaller. With 5×5 pixel window, the results are still quite consistent, whereas with 3×3 pixel window the result appears shows significant randomness.

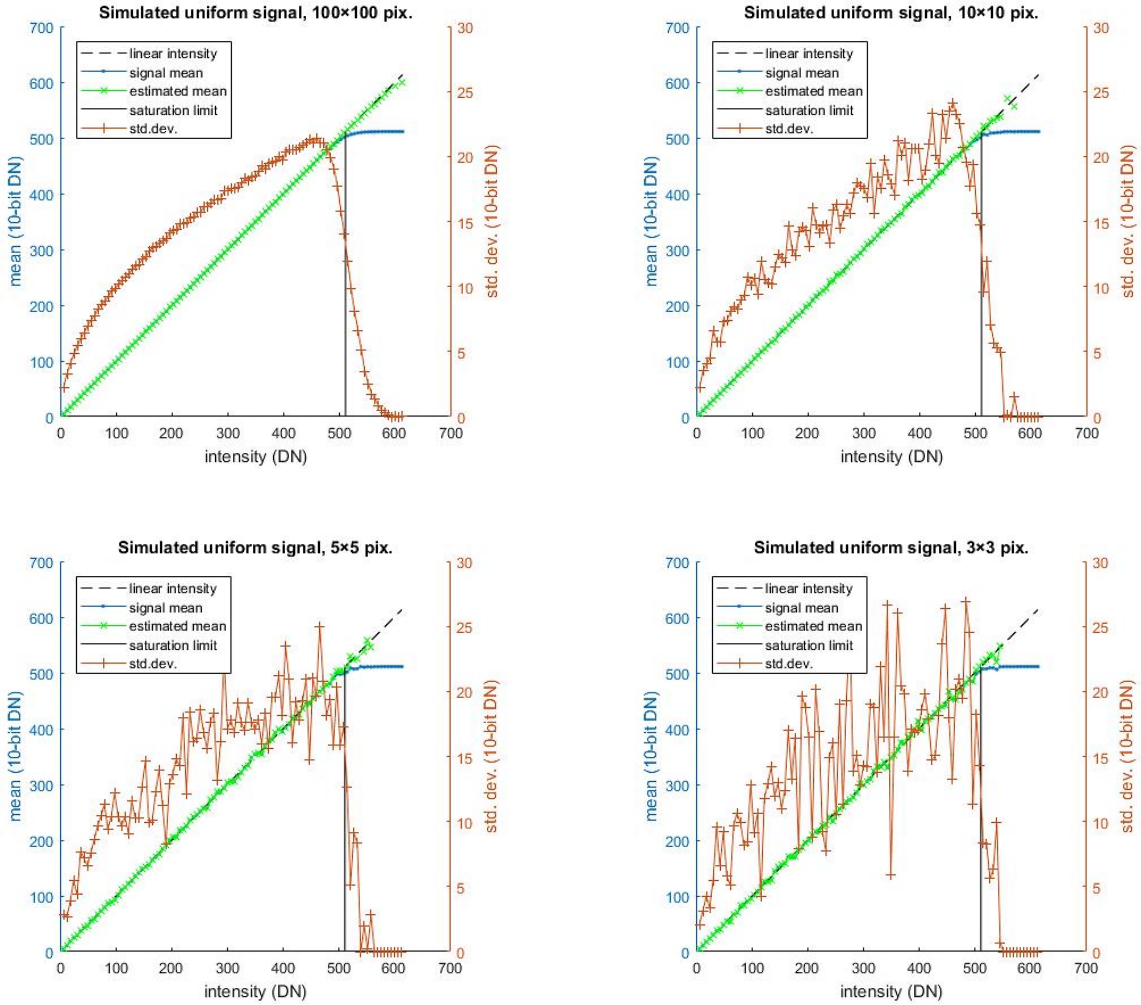


**Figure 4.1: Experimental simulation results with uniform object and Poisson noise.**

In Figure 4.2 experimental results with uniform 10×10 pixel uniform target for 1%, 2%, 5% and 10% Gaussian (normal-distributed) FPN variance are shown. Appearance of FPN is similar to having details in the image, and it can be clearly seen that it interferes with the result. Even with just 1% FPN variance the estimated signal (per equation 3.40) begins to follow the unadjusted local mean, and with 2% FPN variance the estimate actually undershoots the unadjusted local mean. With higher amounts of FPN the result is not helpful anymore.

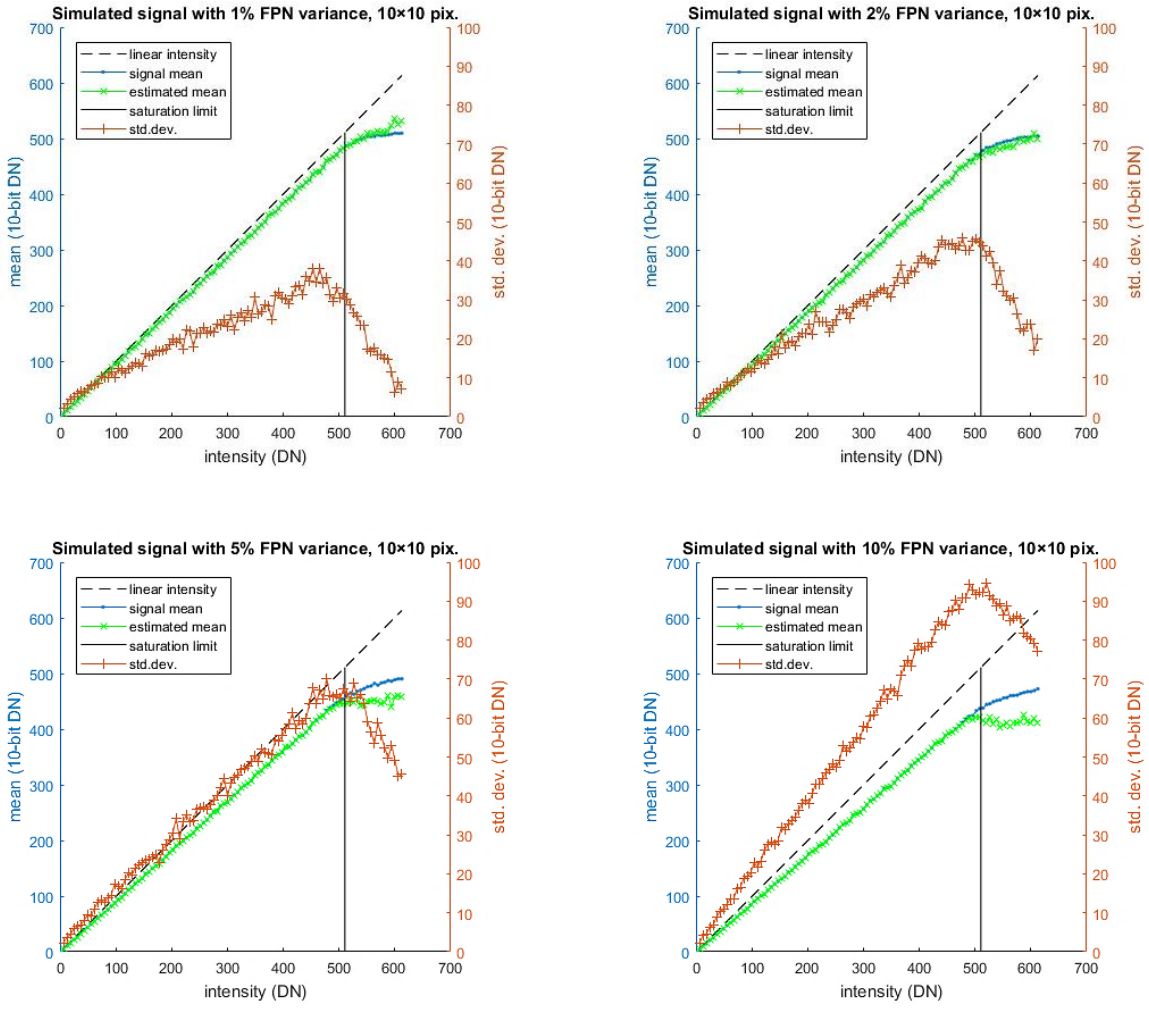


**Figure 4.2: Experimental simulation results with uniform object, Poisson noise and Gaussian FPN.**

It can also be seen how the noise standard deviation indicates that the presence of FPN (or details), as it clearly increases higher than expected for just TN.

# 5 DISCUSSION

In simulation, the method successfully corrects the statistical nonlinearity near saturation, when the degree of local uniformity is high. Equating the actual mean with the estimated mean avoids discontinuity in the estimation, but pulls the result towards the actual mean of the non-saturated pixels when the degree of local uniformity is not very high. After a rather modest deviation from perfect uniformity, the estimate is worse than a simple local mean including saturated pixels as they are. Local uniformity may be decreased due to object details or FPN.

It is vital that the method is accompanied with a way to estimate local uniformity so that the presented method is ran selectively to avoid misestimation of the local mean. This could happen e.g. by comparing an estimated mean of the non-saturated pixels to their actual mean, and using the difference as a weighting between estimated and actual mean. Ideally, FPN should be corrected so that only TN remains in the image.

The presented method can be developed further utilizing the statistical approach established in this work. The requirement of uniformity could be replaced by a variance model which combines noise variance and object variance. Such a model could be based on the actual mean of the non-saturated pixels under a similar statistical analysis. Further, variance, skewness and even kurtosis of the non-saturated pixels could be used to further improve the estimate. A question to keep in mind is, of course, when does the increasing computational cost start to be too high for the benefit. However, it is likely that a useful benefit can be gained even with a somewhat limited, improved model.

Finally, the improved method should be tested on real digital camera images with FPN characterized and compensated for. This thesis presents a core method, but it can be expected that as such it is not yet suitable for real-life application.

# 6 CONCLUSIONS

In this work a method to estimate image local mean for locally uniform objects near saturation was presented. The method overcomes the statistical nonlinearity which occurs when image noise is clipped at saturation, skewing the noise distribution towards lower values. The method was proven to provide a faithful estimate of the local mean under perfect local uniformity, and to improve the local mean under high local uniformity, but to perform worse than simple local mean when the degree of local uniformity decreases below certain level (i.e. when too many details are present locally).

The presented method must be accompanied with another method to estimate the degree of local uniformity to avoid undershoot under low local uniformity. Fixed pattern noise must be accounted for by estimating its contribution, or preferably by correcting for it for before local mean estimation.

The statistical model could likely be improved with reasonable effort and computation cost to combine noise variance with content variance, providing better handling of low uniformity situations.

## REFERENCES


1. Nakamura, J. (editor), Image Sensors and Signal Processing for Digital Still Cameras, Taylor & Francis, USA, 2006
2. Janesick, J.R., Photon Transfer, SPIE Press, USA, 2007
3. Kong, L., Nonlinearity Study of Image Sensors for Mobile Camera Phones, MSc thesis, Tampere: Tampere University of Technology, 2007
4. Darmont, Arnaud, High Dynamic Range Imaging Sensors and Architectures, SPIE press, USA, 2012
5. Holst, G.C., Lomheim, T.S., CMOS/CCD Sensors and Camera Systems, 2nd edition, SPIE Press, USA, 2011
6. Jähne, B., Digital Image Processing, 5th edition, Springer, Germany, 2002
7. Hayter, Anthony, Probability and Statistics for Engineers and Scientists, 4th edition, Brooks/Cole, Cengage Learning, USA, 2012
8. Gonzales, R.C., Woods, R.E., Digital Image Processing, 3rd edition, Pearson, 2010, USA
9. McGraw, T., Fast Bokeh effects using low-rank linear filters, The Visual Computer, May 2014. [Article]. Available: https://www.researchgate.net/publication/271401966_Fast_Bokeh_effects_using_low-rank_linear_filters
10. Tomasi, C., Manduchi, R., Bilateral Filtering for Gray and Color Images, *Proceedings of the 1998 IEEE International Conference on Computer Vision*. Available: http://www.cse.ucsc.edu/~manduchi/Papers/ICCV98.pdf
11. Zhang, X., Brainard, David, H., Estimation of saturated pixel values in digital color imaging, *J Opt Soc Am A Opt Image Sci Vis. 2004 December*
12. IC Insights (2019) Research Bulletin. CMOS Image Sensors Stay on Stairway to Record Revenues. [Online document]. [Cited 2019-09-30]. Available: http://www.icinsights.com/news/bulletins/CMOS-Image-Sensors-Stay-On-Stairway-To-Record-Revenues/
13. Gartner (2019) Number of smartphones sold to end users worldwide from 2007 to 2020 (in million units). Statista. Statista Inc. [Online document]. [Cited 2019-09-30]. Available: https://www.statista.com/statistics/263437/global-smartphone-sales-to-end-users-since-2007/
14. CIPA (2018) Production, Shipment of Digital Still Cameras January-December in 2018. [Online document]. [Cited 2019-09-30]. Available: http://www.cipa.jp/stats/dc-2018_e.html
15. Westland, S., Ripamonti, C., Cheung, V., Computational Colour Science using MATLAB, 2nd edition, Wiley, 2012, UK

16. Andrews, L.C., Special functions of mathematics for engineers, 2nd edition, SPIE Press, 1998, USA